Title
Aluminum Microfoams for Reduced Fuel Consumption and Pollutant Emissions of Transportation Systems

Author
Pilon, Laurent

Publication Date
2008-07-01

Energy Development and Technology 013

"Aluminum Microfoams for Reduced Fuel Consumption and Pollutant Emissions of Transporation Systems"

Laurent Pilon

July 2008

This paper is part of the University of California Energy Institute's (UCEI) Energy Policy and Economics Working Paper Series. UCEI is a multi-campus research unit of the University of California located on the Berkeley campus.

UC Energy Institute
2547 Channing Way
Berkeley, California 94720-5180
www.ucei.org

ALUMINUM MICROFOAMS FOR REDUCED FUEL CONSUMPTION AND POLLUTANT EMISSIONS OF TRANSPORTATION SYSTEMS

UC-EI Award No. 03091156
UCLA Award No. 013038-001

Principal Investigator: **Laurent Pilon**
University of California, Los Angeles
Mechanical and Aerospace Engineering
420 Westwood Plaza, 37-132 Engineering IV
Los Angeles, CA 90095-1597
Phone: (310) 206-5598
Fax. (310) 206-2302
E.mail: pilon@seas.ucla.edu

1. INTRODUCTION

Because of frequent acceleration and slowing down and the high speed of most transportation systems, lightweight structural materials are needed to reduce their energy consumption while maintaining safety. Considering the extensive use of energy intensive transportation systems in the United States even a small increase in energy efficiency will result in significant energy savings and reduction in pollutant emissions. Closed-cell solid foams and microfoams are of particular interest since they are light and feature outstanding combination of mechanical, electrical, acoustic, and thermal properties. They can be used as both structural and functional materials as they present the following advantages:

The closed-cell morphology gives *strength and isotropic mechanical properties* while reducing weight for structural applications.

The presence of air bubbles *reduces the thermal conductivity* which is a desirable feature for thermal insulation and fire retardance.

- Closed-cell foams tend also to *better resist thermal shocks* compared with dense matrix materials (Banhart, 2001).
- Metal foams possess exceptional resistance to impacts *and remarkable strength-to-weight ratio.*
- Closed-cell solid foams possess good acoustic insulating properties.

For all the abovementioned reasons, cellular metallic foams are currently considered for an increasing range of applications including

- **Automotive and Railway Industry.** The increased safety of automobiles has resulted in a higher vehicle weight. However, this conflicts with further demands for low fuel consumption. For example, a car weight reduction of 1% is claimed to give a reduction in fuel consumption of some 0.7% (Banhart, 2001). This would lead to a total reduction of motor gasoline consumption of 1.2 million gallons per day in the US (EIA, DOE, 2002). Lighter cars would also require smaller engines and drive trains resulting in further weight reduction. The chassis' lightweight would be also a tremendous advantage to manufacturers, since weight savings makes parts easier to transport. Moreover the need to reduce acoustic emissions from cars has lead to a demand for new sound absorbers. Metallic foams offer a unique solution for all these problems. Pistons for internal combustion engines made from aluminum microfoams, rather than the more conventional aluminum alloy, would have a higher creep resistance and light weight, thus improving efficiency and reducing emissions. Finally, closed-cell aluminum microfoams are envisioned for defense transport including amphibious vehicles and soldier personal armor (Gama *et al*., 2001).
- **Aeronautical and Aerospace Industry.** In the case of long-range airplanes, the takeoff weight of a Boeing 777-300 varies between 264 and 300 tons (Boeing, 2002) with a consumption of about 100 tons of fuel per flight. Reducing the takeoff weight by 1% would save nearly one ton of fuel per flight (Boris, 1997). Aluminum foams are envisioned in replacement of honeycomb structures in airplanes since they are cheaper and offer the possibility of making composite structures without adhesive bonding. Another important advantage of aluminum sandwiches (aluminum microfoam layer between two aluminum sheets) is that they can be fabricated with curvatures and 3D shapes (Banhart, 2001). Their unique strength-to-weight ratio could also play a key role in fortifying commercial airline cockpits against terrorist attacks, and as structural materials in designing new civilian and military aircrafts.

In space technology, aluminum foam has been evaluated for its use (i) as an energy absorbing crash element for space vehicle landing pads and (ii) as reinforcement for load bearing structures in satellites (Banhart, 2001), (iii) as hyperballistic armor materials for crew quarters or other critical, permanent space installations, and (iv) as acoustic insulation between the spacecraft propulsion system and the crew quarter.

- **Ship Building.** Metal foam can be used not only for main parts of ships but also for naval applications such as elevator platforms, structural bulkheads, antenna platform, and pyrotechnic lockers (Banhart, 2001).
- **Building Industry.** There is also a wide range of possible applications in the building industry. Metal foams can be used for example (i) to reduce the energy consumption of elevators, (ii) as lightweight but strong balustrades of balconies, (iii) as decorative panels.
- **Biomedical Industry.** Titanium microfoams could be used for prostheses or dental implants for example because of their biocompatibility and to ensure ingrowths of tissue.

In order to achieve the desired characteristics of high strength-to-weight ratio and good thermal properties bubbles should (i) be as small as possible, (ii) have a uniform size distribution, and (iii) be uniformly distributed across the aluminum matrix. However, existing methods possesses at least one of the following major drawbacks (1) the bubble are relatively large, typically of the order of a few millimeters in diameter, (2) their size distribution vary significantly, and/or (3) the bubbles are not uniformly distributed across the foam. These issues are even exacerbated when foams are manufactured under microgravity. Then, the metal foam consists of fewer and larger bubbles as shown experimentally by Wübben *et al*.(2003) during parabolic flight.

The present study aims at developing a new, cheap, convenient, and scalable process for producing metal microfoams consisting in closed cells with an average size of 50 microns. By analogy with Colloid Gas Alphorns (CGA) produced from water and surfactant stirred at high speed in a baffled beaker we intend to produce CGA from molten metal. After presenting the state-of-the-art of the different studies carried out on the effect of particles and how to incorporate them in the metallic matrix we will describe the different experiments and the difficulties encountered to introduce the particles in the liquid metal. Finally, we will show that the oxidation of the metal can also play a role in the foam stabilization and metallic foam can be obtained thanks to oxygen injection directly in the metal matrix combined with a high spinning rate. We will see in this part which parameters have to be controlled in order to optimize the process.

2. BACKGROUND

It is impossible to attempt a survey of the vast literature devoted to the study of foams. This section focuses on the physical phenomena occurring in foam.

2.1 Foam Physics

Foams consist of an ensemble of bubbles of different sizes. On Earth, bubbles can take different shapes and polyhedral and spherical bubbles often coexist within the foam layer. The polyhedral bubbles tend to be located at the top of the foam while the spherical ones are at its bottom. Several physical phenomena occur simultaneously or consecutively as the foam is generated. These phenomena are:

- **Gravity drainage** of the liquid through the films and struts separating the bubbles. This phenomenon dominates the foam behavior on Earth and is opposed by viscous forces.
- **Capillary Drainage** of the liquid in the films driven by the capillary pressure due to the curvature of the adjacent Plateau channels and opposed by the disjoining pressure consisting of the Van der Waals attractive forces, the repulsive electrical double layer and the hydration forces (Bhakta and Ruckenstein, 1997). Drainage in the foam eventually stops when the effect of the capillary forces (or Plateau border suction) balances the effect of gravity (Bhakta and Ruckenstein, 1997, Krotov, 1981). Note that capillary drainage does not occur for spherical bubbles.
- **Liquid Film Rupture** leading to the bubble disappearance or to the coalescence of two adjacent bubbles. Coalescence causes the mean bubble size to increase and the number of bubbles as well as the interfacial area of the foam to decrease.
- **Interbubble gas diffusion (or coarsening)** from small bubbles (higher pressure) to large bubbles (lower pressure). This causes the small bubbles to become smaller and the large bubbles to become larger provided that the solubility and the diffusion coefficient of the gas in the liquid phase are large enough. A theoretical analysis by Narsimhan and Ruckenstein (1986) indicates that interbubble gas diffusion is significant only at the top of the foam where the bubble lamellae are thin.
- **Gibbs-Marangoni effect** in thin liquid films and foams results in a decrease of the surface excess surfactant concentration caused by stretching an interface, hence in an increase in surface tension (Gibbs effect), the surface tension gradient thus created causes liquid to flow toward the stretched region, thereby providing both a "healing" force and also a resisting force against further thinning (Marangoni effect).

2.2 Foam Stabilization

2.2.1 Origin of surface tension

The surface tension is due to the anisotropic distribution of the forces sustained by molecules at the surface of a liquid in contact with air. Inside the liquid, all the molecules are subject to attractive forces from the others molecules and the resultant is nil. On the other hand a molecule on the surface sustains an attraction force directed towards the inside of the liquid, since the attraction force of air molecules is negligible (Figure 1). The surface area between the liquid and the air is minimized (Paquot, 2004).

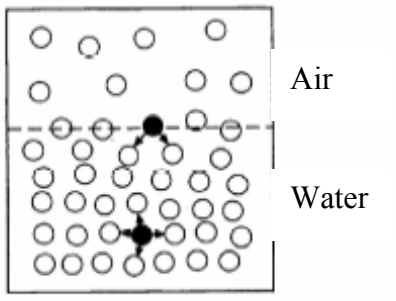

Figure 1. Schematic of the forces sustained by liquid molecules (Paquot,2004).

From a thermodynamic point of view the surface tension, the elementary energy associated with the interface is γdA and $du=Tds - pdv + \gamma dA$. Thus, the energy associated to the interface decreases with a decrease of the surface tension.

2.2.2 Surfactant Properties

A substance is called surfactant when it is able to decrease the surface tension of the liquid/gas or solid/liquid interface. In water, the general structure of a surfactant includes a hydrophilic head and a hydrophobic tail. The hydrophilic end is water-soluble and is usually a polar or ionic group. The interaction nature between water molecules and surfactant molecules is electrostatic. The

hydrophobic end is water-insoluble and is usually a long fatty or hydrocarbon chain. This dual functionality, hydrophobic and hydrophilic, provides the basis for characteristics useful in cleaner and detergent formulations, including surface tension modification, emulsification and foam.

2.2.3 Foam Stabilization by Surfactant

For foam produced with water and surfactants, each bubble of gas or air is surrounded by liquid films. This film is stabilized thanks to the surfactant molecules adsorbed at its surface. The hydrophilic heads interact with water by electrostatic attraction and the hydrophobic tails are in air on both sides of the film. The pressure inside the bubble is larger than that outside and their difference is given by the Young-Laplace equation:

$$\Delta P = P_{in} - P_{out} = 2\gamma\left(\frac{1}{r_1} + \frac{1}{r_2}\right)$$

where r_1 and r_2 are the inner and outer radii of the spherical bubble, P the pressure and γ the surface tension. The pressure difference depends on the bubble size but also in the surface tension. The role of the surfactant is to decrease the surface tension of the water/gas system. As foam is a metastable system that tends to decay with time, lowering surface tension reduces the internal energy of the foams and therefore stabilizes it.

2.2.4 Effect of Particles in Metallic Foam Stabilization

For metallic liquid the stabilization must be different than the aqueous liquid because of the difference of chemistry. Indeed, in liquid metals no surfactants act via electrostatic interaction. The hydrophilic head do not have any electrostatic attraction with the liquid metal. However, it has been observed that the particles help stabilize metallic foams. Their action has been explained in various ways (Wübben *et al*., 2003) as they could

1. Reduce surface tension of a melt and so promote foaminess and foam stabilization. If the surface tension decreases, the energy required to form a gas bubble inside the liquid metal is reduced.
2. Prevent the coalescence of bubbles by separating and consolidating the thin film separating them.
3. Increase the effective viscosity of the liquid metal. Then, the higher viscosity slows the liquid downward flow and thus retards the cell wall rupture process.
4. Have an important impact on foam stability through their attachment to the liquid metal/gas interface (Fig.2) which changes the interfacial curvature and reduces the capillary pressure difference. This capillary pressure difference is the driving force for the draining of the film.

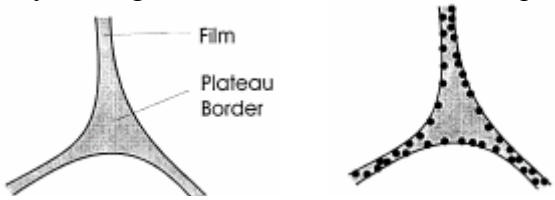

Figure 2. Reduction of the capillary pressure between the plateau border and the tin film by changing the interfacial curvature with the addition of particles (Dequing and Ziyuan, 2003)

Several parameters related to the particles influence the foam stabilization. The following section details the important parameters to consider.

- *Wetabillity of the particles by the molten metal.*

Ip *et al*.(1999) showed that the particles have an optimum effect for foam stabilization when they are partially wetted by the molten metal. Johansson *et al*.(1992) proposed that when the contact angle between the particles and the molten metal at the metal/gas interface is ranging between 40–70°, the

particles have the optimum property for foam stabilization. The measure of the contact angle is shown in Figure 3.

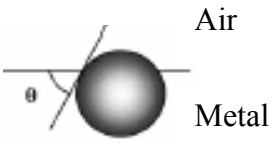

Figure 3. Contact angle between liquid metal and particle (less than 90°) (Binks,*et al*., 2002)

- *Chemical nature of the particle.*

In the elaboration of aluminum foams different particles have been tested suggesting that the chemical nature of the particles plays an important role. Indeed, the contact angle between the liquid metal and the particles depends also on the nature of the particles for a considerate metal. .Usually, carbide (e.g., SiC, BaC) or metal oxide (e.g., Al_2O_3, BiO_2, MnO_2) are used for stabilizing aluminum foam.

- *Particles morphology and concentration.*

Ip *et al*. (1999) showed that foaminess is directly proportional to particle concentration and inversely proportional to particle size. The authors established these results by measuring the life time of the foam while varying the particle size and concentration. They observed that stable foam does not form until a critical particle concentration is reached corresponding to a critical surface coverage (Ip *et al*., 1999). Then, the particles can induce an interfacial separating force (pressure) larger than the sum of cohesion forces stabilizing the liquid-gas interfaces. Moreover, it has been observed that the greater the particle size, the larger the foam cell size produced. In addition, the wall thickness increases with the particle concentration (Dequing and Ziyuan 2003, Babscan *et al*.,2003). These results can be attributed to the fact that smaller particles result in (i) a higher surface coverage of the gas bubble surface, (ii) add strength to the liquid/gas interface, and (iii) are obstacles for liquid flow (Ip *et al*, 1999). The particle shape is also important and spherical particles give better results since their rearrangement is easier due to a better compaction, but usually the particles present a cluster form (Ip *et al*,1999).

2.2.5 Surface Tension and Viscosity of a Liquid Metal

Surface Tension

As explained in section 2.2., lowering the surface tension reduces the internal energy of the foams and therefore stabilizes it. The surface tension of a liquid metal can decrease by adding alloying elements to a pure metal. Some elements are more efficient than others to decrease the surface tension. For example, bismuth showed promising results in lowering the surface tension of molten aluminum. Figure 4 shows the evolution of the surface tension of aluminum/air system as a function of the weight percent of alloying elements between 970 and 1010K. It shows that the temperature of the alloy can also affect the surface tension. For example, for a Bi-Pb alloy, an increase in temperature causes a decrease in surface tension (Giuranno *et al*.,2003).

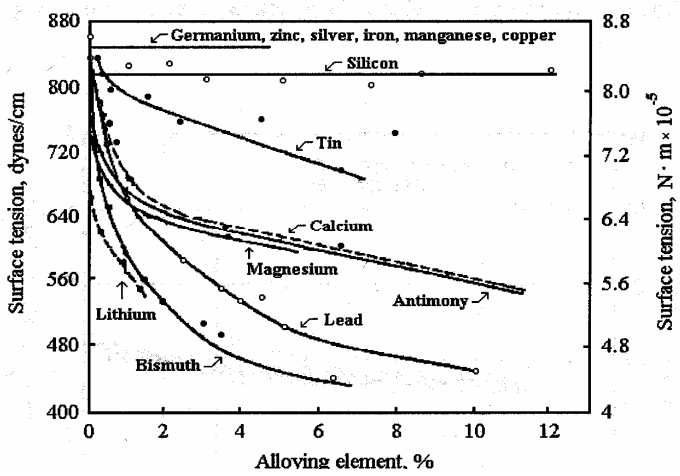

Figure 4. Effects of additives on the surface tension of aluminum at T= 970-1010°K (Hur *et al*., 2003).

Viscosity

The viscosity of an alloy decreases (often exponentially) with the temperature, especially under the liquidus temperature, in a semi-solid state where solid and liquid coexists. The rheological properties of the slurry depend on both the morphology and the proportion of solid phase (Braccini *et al*., 2002).

2.3 Incorporation of particles

The principal difficulty in using particles to stabilize the metal foam resides in introducing solid particles in the molten metallic matrix. This problem is commonly encountered in metal matrix composite elaboration (with aluminum matrix for example). Wetting of the particles by the molten metal however, is essential in incorporating the particles. There are two types of barriers that prevent the incorporation of particles (Hashmin *et al*., 2002):

1. *Mechanics barriers* due to the formation of an oxide film (solid) on the surface. This solid layer is very hard to eliminate and prevents the particles to enter in the liquid phase. Indeed, it creates a mechanical resistance to particle penetration, especially when the particles are added from the top of the molten metal bath.
2. *Thermodynamics barriers* which are usually referred to in terms of wettability. A liquid will wet easily a solid if the solid phase has a higher surface energy than the liquid phase.

This section discusses the different operating and physical parameters enabling particles incorporation.

2.3.1 Wettability and Reactivity in Metal/Oxide Systems

Wetting of oxide substrate by a liquid metal can be divided in two different situations (Eustathopoulos *et al*., 1994):

- *Wetting in non reactive system*. A non reactive system can be defined as a system in which reactivity consists in slight dissolution of the ceramic substrate in the liquid metal, and the maximum amount is in the order of the metallic impurity concentration ((Riviello *et al*., 1994). In this case the wettability is weak (the contact angle is larger than 90º). It has been shown that the wettability can be improved by adding alloying elements in the metal. These alloying elements influence the contact angle by adsorbing at the solid/liquid interface. But in the most favorable case the contact angle remain above 60º (Eustathopoulos *et al*., 1994). One can also note that the oxidation of the liquid metal can drastically decrease the interfacial energy between the liquid and the solid (σ_{SL}) and between the liquid and the vapor (σ_{LV}) surface tension so that the wettabillity is improved.
- *Wetting in reactive system*. In this case the reaction is generally an oxidoreduction reaction at the oxide substrate/liquid metal interface. For example, the reaction of alumina (Al_2O_3) substrate with a molten metal M is the following:

$$3/2\ M + ½\ Al_2O_3 \Leftrightarrow 3/2\ MO + Al$$

The reactivity between the oxide and the metal influences the contact angle. When the reactivity is strong, the wettability of the solid substrate by the molten metal is improved by modification of the interface. A perfect wetting can be expected when at the liquid side, oxygen is adsorb and on solid side a metallic bonded phase is formed. This was observed with the system Ti/MgO (Naidich, 1981). This theory was established by measuring the contact angle of a liquid metal droplet on a solid oxide substrate (Eustathopoulos *et al*., 1994). In the study, we assume that the same phenomenon occurs at the metal oxide particle/liquid metal interface.

2.3.2 Non Eutectic-Alloy in a Semi-Solid State

One of the techniques used to incorporate particles inside a liquid metal during the elaboration of composite materials consists of increasing the viscosity in order to trap the particles added by the top and introduced in the metal matrix thanks to stirring (Suery, 1996). With a pure metal, it is not possible because the viscosity is to low, that is to say of the order of several mPa.s, the particles do not stay in the liquid and rise up on the surface. One can use an alloy which is not in the eutectic composition and presents an interval of solidification instead of a melting point as described in Figure 5. This interval corresponds to the intersection of the two blue lines (for a given temperature and a given composition), in the part liquid plus α phase. In this interval, the alloy is composed of a mixture of solid and liquid phase of which the proportions are given by the inverse segments rule (Suery, 1996).

The viscosity of the two-phase mixture increases with the increasing solid phase fraction and decreasing temperature. As the alloy is cooled with a high mechanical or electromagnetic stirring, the morphology of the solid phase changes. The high stirring can prevent the dendritic solidification and promote the formation of globular solid particles in suspension in the liquid phase (Suery, 1996). The increase in the melt viscosity depends on the shape and the quantity of these solid particles (Braccini *et al*., 2002; Koke and Modigell, 2003; Wu *et al*., 2000). Since the solid particles are more rigid than the fluid against deformation, the particles impose a system of force which will react against the fluid. This resistance increases the apparent viscosity of the fluid. The semisolid "jelly" presents a thixotropic behavior, i.e., the viscosity of the fluid decreases when the shear stress increases. The procedure of incorporation consists of (i) starting from the liquid state, (ii) cooling the alloy with a fast stirring and (iii) introducing the particles when the viscosity is sufficiently high. One keeps stirring to enhance the penetration of the particles in the melt and achieve a homogenous distribution. Then the mixture can be heated again. If the particles have been wetted enough by the alloy, they stick to the liquid metal/gas bubble interface and stay in the liquid metal. Otherwise, they rise back up to the surface. Indeed once the particle is inside the matrix, it is energetically favorable for the particles to become attached to gas bubble, because a particle is never completely wet by the molten metal, and the energy needed to stay at the liquid metal/gas bubble interface is lower (Hashim *et al*., 2002).

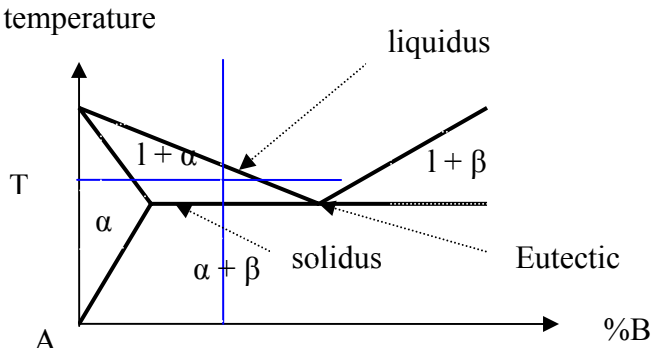

Figure 5. Phase diagram of an alloy A-B

2.3.3 Interaction of Particles with Dentritic Solid-Liquid Interface

As we explain previously, the solidification of a non-eutectic alloy accompanied by a high mechanical stirring can lead to a microstructure formed of globular particles in suspension in the liquid metal. However, it is also interesting to consider a dendritic microstructure if the globular microstructure is not totally obtained. Different theories have been proposed to describe the interactions between insoluble particles and advancing solid/liquid interface (Kurian and Sasikumar, 1991; Wilde and Perepezko, 1999). The possible interaction modes are illustrated in the Figure 6.

- Pushing: the particles are pushed by the growing dendrites and get entrapped in the interdendritic eutectic (Kurian and Sasikumar, 1991).
- Entrapment: The particles are trapped in the dendritic network due to the growth of secondary arms (Kurian and Sasikumar, 1991).
- Engulfment: The particles prevent the reject of solute that causes a decrease of the critical solidification velocity. That implies that the particles should be in a solidifying alloy melt should be engulfed by the primary phase when the particles come in to contact with it. (Kurian and Sasikumar, 1991).

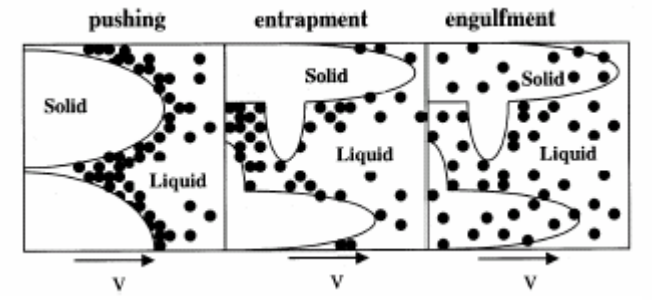

Figure 6. Schematic illustration of the possible interactions modes of a dendritic solid/liquid interface with dispersed foreign particles (Wilde and Perepezko, 1999).

Moreover, the particle distribution in slurry under dynamic condition of flow is influenced by the particles size (Hashim *et al*., 2002):

- For particles smaller than 10 μm in diameter, the effect of gravity is negligible and they are carried in suspension in the liquid. In other words, the particles do not accumulate at the bottom of the beaker due to their density larger than the one of the liquid phase. Thus, the particles are uniformly distributed across the melt.
- For particles above 10 μm, the gravitational effect is not negligible and a particle concentration gradient will develop, and some particles sedimentation takes place.

To obtain metal microfoam we speculate that particles should have radius less than 1 μm so that they remain much smaller than the bubbles.

2.3.4 Operating Parameters

More generally, the following parameters have to be taken into consideration in order to control the introduction of non metallic particles in a molten metal (Asthana, 1993):

- *Alloy chemical composition.*
- *Particle temperature* because some local solidification can be induced by the cold particles.
- *Stirring rate*: Since wettability of ceramic reinforcement by molten metal is poor, an external driving force is required to overcome the surface barriers. This force can be provided by a mechanic or electromagnetic stirring. There is a minimum rate to incorporate the particles (Dequing and Ziyuan, 2003, Tham *et al*., 1999). For example, incorporation of SiC particles in an aluminum matrix is enhanced by increasing the stirring speed. Then, the particles floating on the surface are drawn toward the center and then fall in the vortex created by the propeller and can be introduced into the liquid.
- *The temperature of the molten metal*. It is easier to incorporate particles in a semi-solid state by increasing the viscosity and trapping the particles (Suery, 1996).
- *Particle agglomerates* must be broken up before complete dispersion and wetting can occur. The particle aggregates tend to promote the flotation due to their surface area and prevent the incorporation in the metal matrix (Hashim *et al*., 2002).

2.4 Closed-cell foam manufacturing process

Existing synthesis path for closed-cell aluminum (macro) foams have been recently reviewed by Banhart (2001). In brief, they can be manufactured by the following liquid or solid state processing:

Liquid State Processing

- *Blowing agent foaming*. Instead of gas bubbles, blowing agents are added to molten aluminum. Under high temperature, the blowing agent decomposes, generates gases, and forms bubbles.
- *Solid-gas eutectic solidification (gasar).* Aluminum is melted under hydrogen atmosphere that dissolves and saturates the melt. Upon cooling the liquid phase undergoes a eutectic transition (liquid→ gas + solid) to form foam.
- *Powder compact melting*. A blowing agent is mixed to aluminum powder. The mixture is then compacted, worked, and shaped (cut). Upon thermal treatment above the melting temperature, the blowing agent decomposed into gas and aluminum foam is formed.
- *Heating a metal with a volatile one (Sosnick, 1948).* Aluminum and mercury are mixed in pressure vessel. The increase of the temperature allows volatilization of mercury and the melting of aluminum. The aluminum melt is supersaturated with mercury gas. However, this process was not commercially successful.

Solid State Processing

- *Slurry foaming.* The slurry consists of aluminum powder, gas blowing agent, and additives. The slurry is heated below the melting temperature where it turns viscous due to the additive and expands due to the decomposition of the blowing agent. The expanded slurry is then dried and sintered yielding aluminum foam.

Table 1 summarizes the characteristics of the closed-cell aluminum foams produced under earth gravity from the above processes.

Table 1: Summary of the morphological properties of aluminum foams produced by existing synthesis methods (Banhart, 2001)

Process	Foam density (g/cm^3)	Pore size (mm)	Size Distribution	Porosity	Comments
Gas injection	0.069 to 0.54	3 to 25	Non-uniform	80 to 98%	Commercially available
Blowing agent	0.18 to 0.24	2 to 10	Non-uniform	90%	Commercially available
Gasar	0.6 to 2.6	0.01 to 10	Highly non-uniform	5 to 75%	Not available commercially
Compact powder melting	0.28 to 1.1	1 to 20	Highly non-uniform	60 to 90%	Commercially available
Slurry foaming	> 0.20	N/A	Non-uniform	<93%	Insufficient strength - cracks in the foam

Note that other manufacturing processes for closed-cell metal foams exist but for different materials such as titanium, zinc, magnesium, copper, and steel. For example, metal foams can be formed by incorporating ceramic hollow spheres in a liquid metal.

Recently, Wübben *et al*. (2003) generated lead foams on Earth and under microgravity conditions during parabolic flight from lead powders having two different oxide contents. Lead alloys have been used as a model material for aluminum foaming in space. Gas bubbles were generated by a gas-releasing agent and the foaming process was observed in-situ by X-ray radioscopy. The authors concluded that the main function of the powder is to inhibit bubble coalescence. They also noted that foams generated in microgravity have fewer and larger bubbles.

To conclude, existing manufacturing processes of closed-cell solid foams seem to have significant drawbacks including (i) a lack of repeatability, (ii) large bubbles, and (iii) non-uniform morphology of the foam produced. These drawbacks are exacerbated under microgravity as experimentally demonstrated by Wübben *et al*. (2003).

2.5 Colloidal Gas Aphrons or Microfoams

Colloidal Gas Aphrons (CGA), also called microfoams, consist of bubbles between 25 and 50 μm in diameter with a porosity of up to 60%. They can be produced by stirring an aqueous surfactant solution contained in a fully baffled beaker at room temperature, as described in Figure 7 (Sebba, 1987).

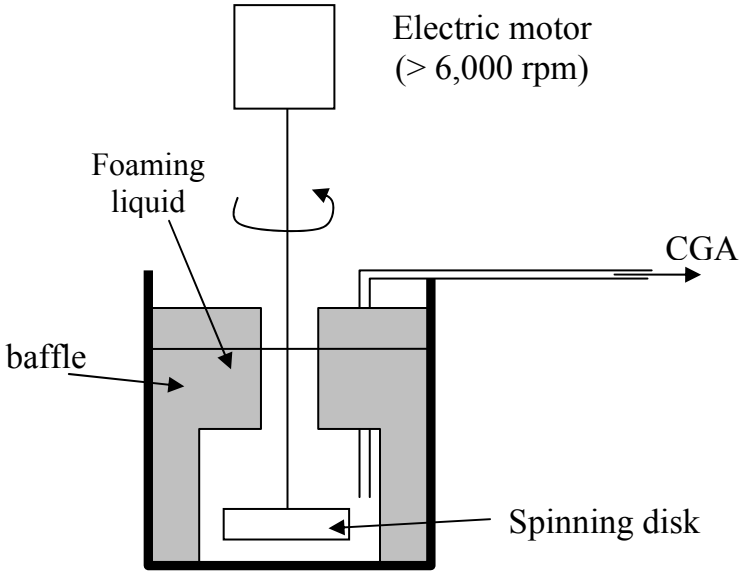

Figure 7: Detailed schematic of the CGA forming process

The solution is stirred by a spinning disk driven at 5,000-10,000 rpm by an electrical motor. Two to four baffles are equally spaced around the container and extend well above the surface of the solution. Once a critical stirring speed has been reached, waves are produced at the liquid surface. The waves beat up against the baffles, and having nowhere else to go, re-enter the liquid at the baffles. It is believed that the re-entering liquid carries a thin film of gas which becomes sandwiched between the liquid and the baffle. Such a thin film is unstable and breaks into microscopic bubbles encapsulated by a soapy shell, i.e. minute gas aphrons. After a few minutes of stirring, a CGA forms and rises at the surface of the solution. It has been reported that CGAs made of water and surfactant solutions:

- have stable bubbles with a narrow and reproducible size distribution between 25 and 50 μm (see Figure 8)
- exhibit high stability,
- separate easily from the bulk liquid phase, and
- have similar flow properties to those of the liquid phase.

Colloidal Gas Aphrons are subject to the same physical phenomena as those taking place in foams and described earlier. Since bubbles are spherical and highly stable (see Figure 8b), capillary drainage does not occur. Moreover, on Earth the effect of buoyancy caused by the density difference between the gas and the liquid phases is relatively limited due to the small size of the bubbles. Then, microbubbles act as a colloidal suspension and the effect of gravity is not as dominant as in foams.

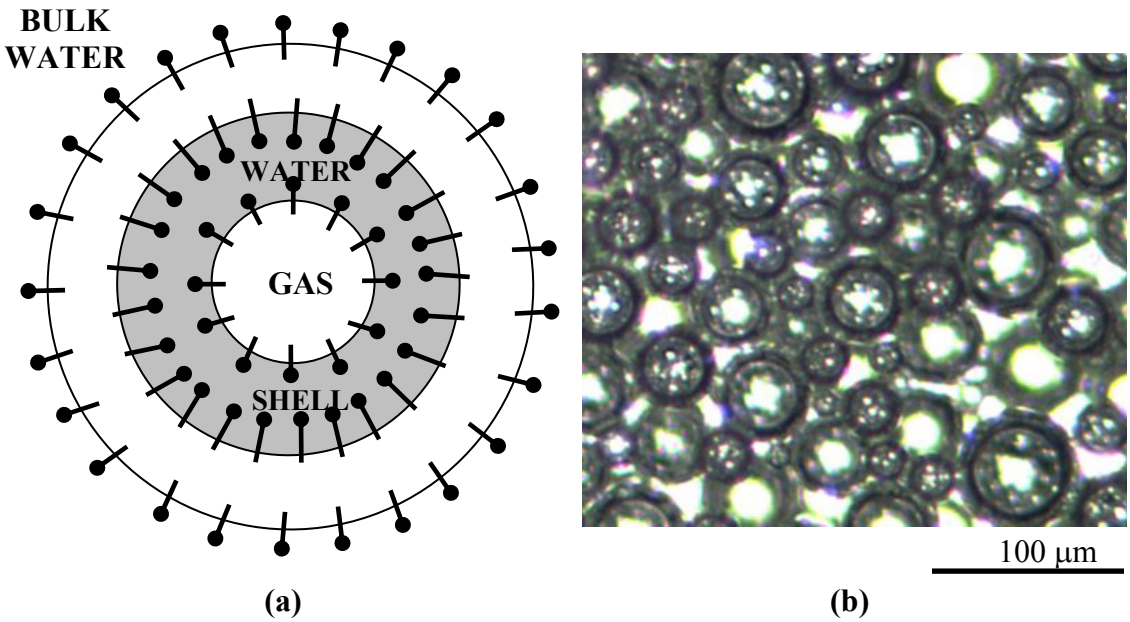

Figure 8. Microbubble with encapsulating soap film in aqueous Colloidal Gas Aphrons (a) schematic diagram proposed by Sebba, 1987, (b) micrograph taken in the PI's laboratory

There are still many unresolved questions regarding the formation and the structure of Colloidal Gas Aphrons (Sebba, 1987). Explanation regarding their formation and structure are still speculative. The most widely accepted structure speculates that bubbles have a multilayered shell as shown in Figure 8a but no direct observation or physical models have demonstrated such a structure. Until now, CGAs have been produced only from low viscosity aqueous solutions at room temperature. In this case, the presence of surfactant is required. Surfactants are also necessary to generated (macro) foams from low viscosity fluids such as water. Figure 8b shows photograph of CGA samples taken at the inlet and outlet of the test section and observed under a Leica DM IL microscope.

3. EXPERIMENTS

This section presents the experimental strategy, apparatus, and procedure followed during the course of the study. The materials and instruments used are described in details.

3.1 Experimental Strategy

3.1.1 Objectives and Strategy

The objective of this study was to produce solid microfoam with an average cell diameter less than 100 μm using CGA process used to produce aqueous CGA. Such materials would be light and strong for applications ranging from structural materials and shock absorbers in various transportation systems from airplanes to cars and elevators. At the start of the project, it was unclear whether such a process could produce foams at all, let alone foam with micrometric cells.

Several strategies have been explored. First, oxide particles with various diameters and in various concentrations were used to act as surfactants, stabilize the microfoams, and prevent bubble coalescence. Mixtures of air and inert gas such as argon were also injected directly in the molten metal to oxidizing the bubble wall in a controlled manner. The melt was stirred at high speed in a fully baffled beaker in order to break the large bubbles and entrapped air in small bubbles forming from the waves breaking against the baffles.

3.1.2 Raw Materials

In current aerospace technologies, aluminum alloys are the materials of choice for most structural applications. Aluminum presents the advantages of being very light and strong and has large thermal and electrical conductivities. Its melting temperature is relatively low (650^{o}C) and it has a large thermal expansion coefficient. For example, hundred of tons of aluminum from spent boosters and old satellites are orbiting Earth. These orbiting objects are hazardous as they may collide and damage orbiting satellites. However, recycling of this material would reduce the hazards and offer a potential attractive source of aluminum to be recycled. However, for the sake of simplicity during the process development, we chose to work with tin, tin alloys and bismuth alloys instead of aluminum because of their low melting temperature (70ºC < $T_{melting}$ < 250ºC). The relatively high temperature required for melting aluminum could damage the equipments and it is easier to work at low temperature and to find the proper cooling experimental apparatus. However we expect aluminum alloys to feature the same behavior as tin and bismuth alloys.

Table 2. The different alloys used for the development of the process.

	Alloy 1	**Alloy 2**	**Alloy 3**
Alloy composition	42.5% Bi, 37.7% Pb, 11.3% Sn, 8.5% Ca	40% Sn 60% Pb	48% Bi, 28.5% Pb, 14.5% Sn, 9% Sb
Specific gravity	9.4	9.3	9.5
Semi-solid state temperature window	70-88^{o}C	182-257^{o}C	102-226^{o}C
Tensile strength	1.12 MPa	38 MPa	1.65 MPa
% elongation in slow loading	220%	35%	<1%
Brinell hardness	9	15.8	19
Maximum growth after casting (mm/mm)	+ 0.025	N/A	+0.061

Moreover, the alloys used in the present study are not at the eutectic composition and therefore present a favorable interval of solidification. Table 2 summarizes the composition of the different alloys studied and their melting temperature interval along with their specific gravity. These materials have been chosen for their low melting temperature. Moreover, they are used as solder material as they wet most of metal surfaces. For example, for a Sn-Pb-Bi alloy, an increase of the weight percent of bismuth and lead components decreases the surface tension of the liquid alloy/air interface (Prasad and Mikula, 1999, Guiaranno *et al*., 2003). Note that, some experiments have also been performed with pure tin in order to test the effect of the matrix composition on the foaming process.

Table 3 summarizes the size and density of the particles used to stabilize the foam including Bi_2O_3, SnO_2, CeO_2, SiC, TiC, and stainless steel. These particles were chosen to study the effect of the following parameters:

1. gravity: the oxide particles have a specific gravity bigger or in the same order than the one of the tin (specific gravity: 7.2)
2. The particle size which ranges from 80 nm to 45 μm
3. The effect of the chemical composition of the particle: the wettability of the particles depends on the chemical nature of both the liquid metal and the particles. With the oxide particles, the kind of reaction described in the section 2.3.1. can be expected. Carbides and oxides are usually used for aluminum foam stabilization. Stainless steel powder was chosen as an alternative solution, indeed these particles are metallic and the alloys presented in Table 2 should wet easier these particles since they are used to weld metal pieces together.

Table 3. Summary of the properties of particles used to stabilize the foam.

Nature of particles	Average diameter	Specific gravity
Bismuth oxide	150 nm	8.2-8.9
Tin oxide	80 nm	6.6-6.9
Cerium oxide	80 nm	7.2
Silicon carbide	1 μm	3.2
Titanium carbide	2 μm	4.9
Stainless steel	45 μm	8

3.1.3 Experimental Setup

Figure 9 shows the experimental setup used in the present study. It consisted of a stainless steel container with molten metal heated by a commercially available heating mantle or a Fisher Scientific Isotemp™ hot plate. The Silverson LT4R mixer could reach a speed of 10,000 rpm. The baffles, the stirring propeller, and the shaft are made of stainless steel 316. The container was sealed with an aluminum lid featuring a hole to accommodate the stainless steel shaft. Additional openings accommodated (1) an inert gas inlet, (2) a gas outlet to maintain atmospheric pressure in the chamber, and (3) a thermocouple to monitor the melt temperature. The atmosphere content above the melt was controlled to avoid oxidation thanks to Argon flushed into the chamber. The gas flow rate was measured using a Harris flow meter, model 325-2. Argon gas was injected directly in the molten metal and the temperature of the gas was controlled by an electrical resistance (AHP, OMEGA). The quantity of gas entrapped due to the stirring and the baffles may not be sufficient to achieve a high porosity and direct injection of gas may help to form the foam. The baffles may also break the biggest bubbles into smaller ones. The temperature of the gas was measured as a function of the tension of the variac for an argon flow of 2360 cm^3/min. The inlet and the outlet temperatures were measured with a Fisherbrand™ "traceable" thermometer equipped with a type-K thermocouple. The temperature of the gas was measured as a function of variac tension for an argon flow of 2360 cm^3/min.

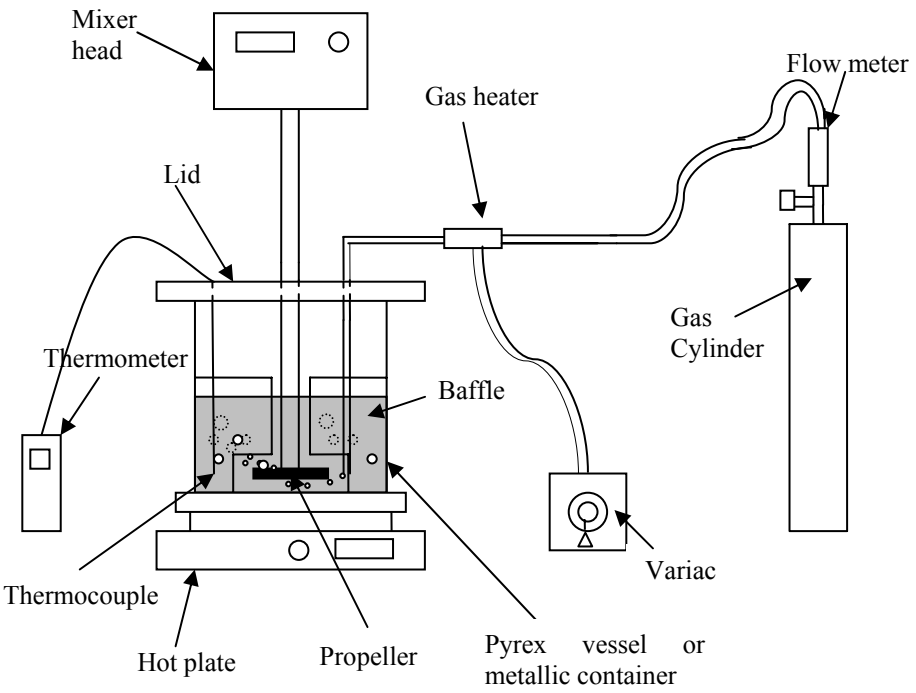

Figure 9. Schematic of the experimental setup assembled at UCLA.

3.2 Experimental procedure

3.2.1 Incorporation of Particles in Pure Tin Melt

As described in Section 2, particles play an important role in the success of existing elaboration processes of metallic foams. Indeed, in the Alcan and Cymat processes (Barnhart, 2001), 5 to 15 vol.% of particles smaller than 20μm are introduced to make the molten metal sufficiently viscous for molten liquid foams to be stable. As explained previously, the stabilization occurs thanks to several phenomena including (i) increase in the melt viscosity, (ii) prevention of bubble coalescence, and (iii) reduction of surface tension. Introducing particles into a metallic matrix is a difficult process and different parameters must be taken into consideration: (i) stirring rate, (ii) temperature of the molten metal, (iii) temperature of the particles, (iiii) temperature of the argon atmosphere.

In order to introduce the oxides particles (Table 3) in pure liquid tin, the following parameters were tested for different values of (i) stirring speed, (ii) melt temperature, (iii) initial particles temperature, and (iv) temperature of the argon atmosphere. Many precautions were taken to prevent the formation of the oxide layer at the surface of the melt by operating under argon atmosphere and by polishing the blocks of tin prior to melting.

Moreover, a different experimental process was carried out using a mixture of pure tin powder and bismuth oxide powder. First the two powders were well mixed by manually shaking the container. The mixed powders were then transferred into an alumina crucible and heated at 350ºC under Argon atmosphere.

3.2.2 Particle Incorporation with Bismuth and Tin Alloys

In order to simplify the experiment setup we selected alloys featuring a melting temperature lower than that of pure tin (230^{o}C). Simultaneously, we could explore the effect of alloying on the foaming behavior of liquid metal. In addition, particles are known to be introduced more easily in the semi-solid state (Suery, 1996). The method used to introduce the particles was the following:

- The liquid was heated above the liquidus temperature and stirred under argon atmosphere to prevent the oxidation. Some experiments were carried out without the lid in air.
- Heating was stopped and the metal was cooled while continuing stirring until the temperature interval of the semi-solid state.
- Then, the particles were introduced progressively from the free surface of the melt.

3.2.3 Stabilization by Oxidation

Riviello *et al*.(1994) described an experimental setup similar to that used in the present study. The authors used bismuth alloy (50% bismuth, 25% lead, 12.5% cadmium and 12.5% tin) and tin alloys (50/50 lead-tin solder) to produce powders using the CGA process (Sebba, 1987). First the molten metal was stirred and the air was entrained inside. Metal foam was formed with bubbles on the order of 50 to 100 microns. The surface tension of the molten metal acts on the thin lamellae oxidized by the air entrapped. These lamellae break under the action of the high surface tension stretching the film and form particles. In order to understand the effect of oxygen in the foam stabilization we performed the following experiments:

1) The liquid metal was stirred in an inert atmosphere and a hot argon flow was directly injected inside the melt. The same experiment was also run in air atmosphere and compared with the previous one.

2) A mixture of air and argon flow was directly injected in the molten metal. To control the quantity of oxygen in the flow of argon the setup shown in Figure 10 was developed.

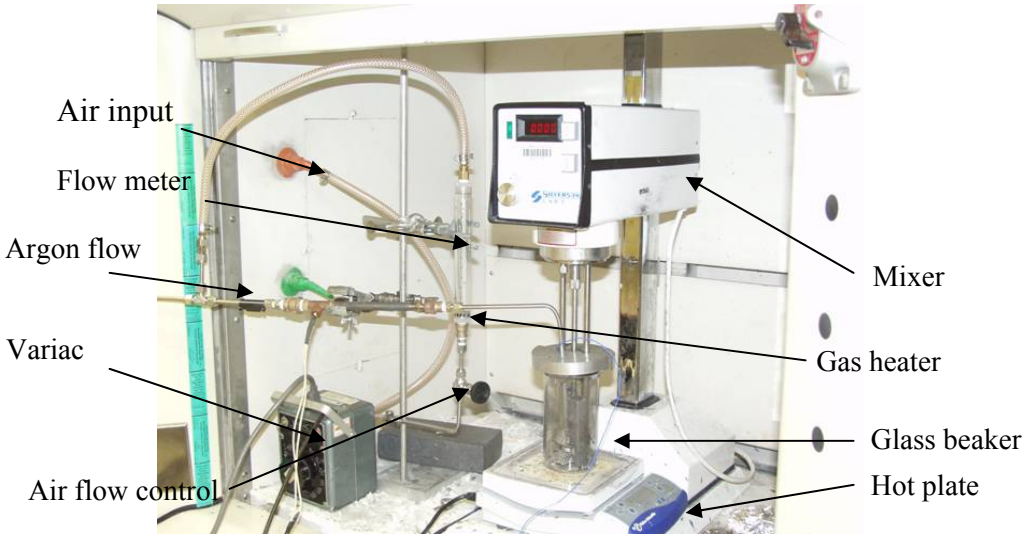

Figure 10. Experimental setup to control the quantity of oxygen in the gas flow

In these set of experiments, the solid metal was cut in small pieces and put in a sealed beaker. The metal was heated thanks to the Fisher Isotemp™ hot plate. The flow of argon was controlled by the flowmeter Harris 325-2 while that of air was controlled thanks to a flowmeter Omega FL-112 β.

Then, the gas mixture was heated by the electrical resistance system (AHP, OMEGA). The experimental results are reported in Section 4 where the effects of key parameters on the foaming process are discussed in details.

4. RESULTS AND DISCUSSION

This section presents the experimental results regarding incorporation of particles in molten tin as well as in bismuth-tin alloys. The effects of the following operating parameters will be discussed including (i) particle size, (ii) alloy temperature, (iii) particle specific gravity, (iv) the working atmosphere. In a second part the experimental result on the experiments perform to realize the effect of oxygen in the foam stabilization will be detailed and the key parameters will be discussed.

4.1 Incorporation of Particles

4.1.1 Experimental Results

Pure Tin and Oxide Powder

To incorporate oxide particles in pure tin the operating parameters were varied as follows:

- stirring rate: from 0 to 8,000 rpm.
- temperature of the molten metal: from 230 to 400ºC (the melting temperature of pure Sn is 230ºC).
- temperature of the particles at the introducing time: at room temperature or at the same temperature as that of the molten metal.
- temperature of the argon atmosphere : at room temperature or at about 100ºC.

In all cases, the particles floated at the liquid metal surface even if their density was higher than that of the metal. Note that despite many precautions, a thin oxidation layer was always present at the molten metal surface.

To try to bypass this difficulty, a different experimental process was carried out with a mixture of pure tin powder and bismuth oxide powder. First the two powders were mixed by manually shaking the container. The mixed powders were then transferred into an alumina crucible and heated at 350ºC under Argon atmosphere. After heating for one hour, we observed a crust on surface of liquid tin. This crust consisted of unmolten tin particles and unwetted bismuth oxide particles. The bismuth oxide particles were not incorporated with the liquid tin. We could find these particles on the surface or between the liquid metal and the crucible walls. The melting of the tin particles at the top of the melt was likely made impossible by the presence of the oxide layer naturally forming at the surface.

From this series of experiments several questions remain unanswered:

- Were the right particles selected? The contact angle between the liquid metal and the particle was large and so the particles might not be wetted by the liquid metal. However, it is difficult to measure the contact angle of these microparticles with molten metals.
- The use of a non-eutectic alloy may be a better solution than the pure tin as it is easier to incorporate the particles in the semi-solid state as previously discussed in Section 2.2.2.

Particles Incorporation with Bismuth and Tin Alloys

The different parameters explored for each experiment are presented in the table 4. The results can be summarized as follows:

- Stainless particles were successfully introduced in Alloy 1 either in liquid and semi-solid state and either in argon and air atmosphere (Experiments 5 and 6).
- The silicon carbide particles were successfully incorporated in Alloy 1 in a much oxidized state (Experiment 8). Indeed, some air was directly injected in the metal prior to adding the particles and the metal became very viscous. Then the metal matrix composite was cooled. It was heated up again at 120ºC and stirred at 5000 rpm with a direct argon injection. But only the liquid around the propeller was stirred and the fluid on the sides did not follow the movement because the viscosity was too high.

Table 4. Parameters explored for incorporating particles into the alloy matrix.

Experiment #	1	2	3	4	5	6	7	8
Alloy	2	2	2	1	1	1	1	1
Particle type	TiC	SiC	TiO_2	BiO	Stainless	Stainless	SiC	SiC
Particle Size (μm)	2 μm	1 μm	0.8 μm	0.15 μm	< 45 μm	< 45 μm	1 μm	1 μm
Particle Specific gravity	4.9	3.2	6.6-6.9	8.2-8.9	8	8	3.2	3.2
Atmosphere	Ar	Ar	Ar	Ar	Ar	air	Ar	air *
Particle Temperature	25ºC	25ºC	25ºC	90ºC	90ºC	25ºC	90ºC	25ºC
Melt temperature	230ºC	220ºC	220ºC	80ºC	80ºC	120ºC	80ºC	120ºC
Stirring Rate (rpm)	4000	4000	4000	5000	5000	5000	6000	5000
Particle incorporation?	no	no	no	no	yes	yes	no	yes

4.1.2 Discussion

From the experimental results, one can draw the following conclusions:

- Only the stainless particles have been incorporated into the molten metal. These particles are bigger than the oxides and the carbides (10-45 μm) and do not form aggregates like the nano-powders as observed under the microscope.
- The size of the particles plays an important role and if one refers to the description of the gas injection process made by Banhart (2001), the size of the particles added to the liquid metal ranged between 5 and 20 μm. Therefore, one can assume that particles less than 5 μm are very difficult to introduce regardless of their chemical nature: neither oxides nor carbides were successfully introduced in the molten alloys. Additional experiments should be performed with oxides and carbides particles with the size ranging from 5 to 20 μm in diameter to confirm this assumption.
- silicon carbide particles 1μm in diameter have been incorporated in a highly oxidized liquid Alloy 1. The oxidation decreases the surface tension but the mixture was too viscous to be stirred at high speed. The same experiments should be run for Alloy 3.

4.2 Oxidation Stabilization

This section presents the experimental results and discusses the effect of the different parameters influencing foam stabilization.

4.2.1 Experimental Results

Effect of Oxygen

We tried to produce foam and stabilize it thanks to oxidation of one or several of the elements of the alloys. The metal was melted at 100ºC. Then, it the molten metal was stirred and hot argon was simultaneously injected at about 100ºC. This experiment was first done in air. Formation of bubbles at the melt surface could be observed. When Ar gas was injected, the level of liquid metal raised. However, when Ar injection stopped, the foam layer fell down. The rise on the melt could be due to:

- The formation of foam, but this foam was not stable and quickly decayed.
- A large pocket of gas may have formed under the free surface. Due to the high surface tension of the liquid metal, the bubbles are unstable and coalesce easily thus forming a gas pocket.

To understand the effect of oxygen, the same experiment was carried out with a lid preventing the oxygen from entering the chamber thus, keeping an inert environment above the melt. In these conditions the metal did not foam, it was not possible to stir the metal at more than 3,000 rpm without creating random splashes in the liquid metal. Heating the argon gas (around 100ºC) and injecting it in the molten metal did not cause more bubbles or foams to form.
However, as soon as the lid was open to the ambient air, some oxygen could enter the chamber and the metal foamed almost instantaneously. The metal could be stirred at 8,000 rpm without the splashing previously seen. The foam formation was concentrated around the baffles. After stirring for 6 minutes, black powder was released from the melt free surface. The powder was likely formed according to the mechanism previously discussed and exploited by Rivierro *et al*.(1994) to generate tin powder.
These experimental observations indicate that air was entrained into the melt due to the stirring. Moreover, we speculate that the foam was stabilized thanks to the formation of an oxide layer formed at the surface of the bubbles.

Control of Oxygen Amount in the Gas Flow

This experiment was first carried out with Alloy 1.The liquid metal was heated up to 120ºC in a hot argon atmosphere (100ºC). Then the flow of argon (2360 cc/min) was directly injected in the molten metal stirred at 2,000 rpm. A flow of air was mixed with the argon flow at 180 cc/min. This corresponds to 1.6 vol.% of oxygen in the argon flow if we consider that the air is composed of 21% of oxygen. Note that beyond 2,000 rpm the liquid metal splashed. The following events were observed:

- After 30 seconds from the gas mixture injection start, the stirring rate was increased to 5,000 rpm.
- After 1 minute we could reach the rate of 8,000 rpm without metal splashing.
- After 2 minutes, a 2.5 cm thick foam layer was formed. This one remained stable for 10 s and was broken by a wave of liquid metal.
- After 5 min 30 s of stirring the surface became covered with black powder rising up from the melt and reaching the lid.
- At this time, the stirring and the gas injection were stopped and we waited for 5 min. Then, the experiment was run again and a stirring rate of 7,000 rpm.

A very stable 3.5 cm thickness was formed. This foam was solidified and it appeared that it was much more oxidized and therefore very brittle. Figure 11 shows the cellular structure of this foam.

The same experiment was run with cold argon directly injected in the metal and a progressive injection of air in the chamber above the melt thanks to a syringe. This experiment led to the formation of a thin layer of foam (~ 0.5 cm), and underneath a large pocket of air was formed as shown in Figure 12.

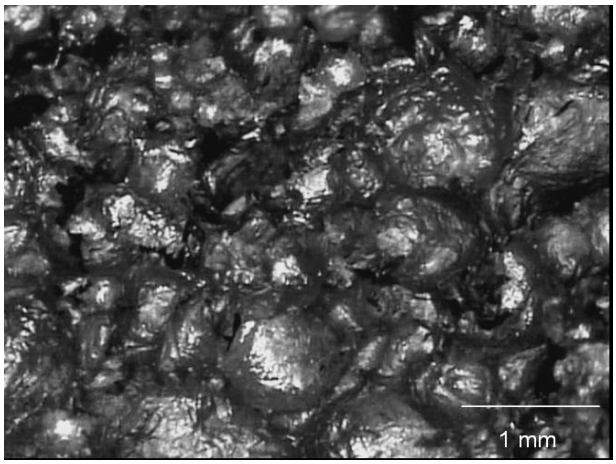

Figure 11. Foam formed with a high level of oxidation

Figure 12. Gas pocket formed in the liquid metal around the propeller. This state was solidified by liquid nitrogen.

Foaming in the Semi-Solid State

Alloy 3 was heated up to 230ºC in air. Once that temperature was reached, heating was stopped and stirring at 3000 rpm started. Quickly (after 2 minutes), some black powder was released at the free surface. We stopped the air injection and we kept cooling the alloy while stirring at 2000 rpm to limit the release of black powder which decreased with the cooling of the melt. At about 150ºC, the release of powder stopped. At this temperature the alloy was in the semi-solid interval (102-226◦C). Then, only cold air was injected in the melt at a flow rate of 200 cc/min and at 25ºC. The melt was stirred at about 6,000 rpm for 3 minutes and a 6 cm thick stable foam was formed. We stopped the stirring and we let the foam cool down. Figure 12 shows the foam obtained. It is evident that the bubbles diameter increases from the bottom (500 microns to 5 mm) to the top (about 7 mm). This can be attributed to bubble coalescence. Unlike the foam sample obtained with Alloy 1, this foam is not brittle.

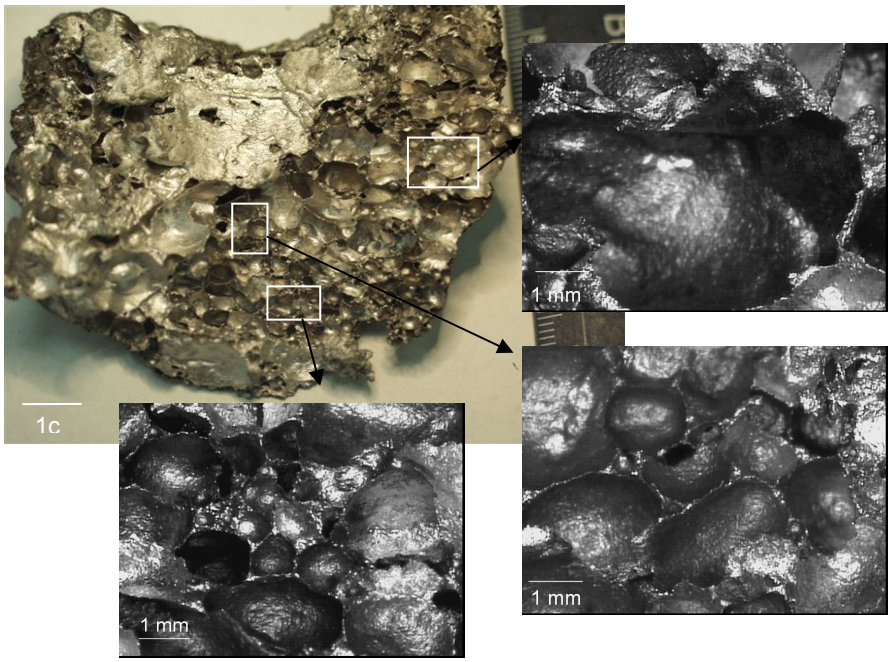

Figure 12. Metallic foam formed from Alloy 3.

4.2.2 Discussion

A metal is naturally covered by a film of its oxide that prevents it from further oxidation in air. This "protective skin" develops by the following steps schematically illustrated in Figure 13 (Addepalli *et al*., 2000). First, the molecules of oxygen are first adsorbed by physisorption, and then more

strongly attached to the metal by chemisorption. A small oxide nucleus is formed on the surface by the followings electrochemical reactions,

$$M \rightarrow M^{y+} + y\, e^-$$
$$\tfrac{1}{2}O_2 + 2e^- \rightarrow O^{2-}$$
$$x\, M + \tfrac{1}{2}\,(yO_2) \rightarrow M_xO_y$$

The oxide nuclei grow and eventually form a continuous oxide film. The equilibrium constant of the above reaction is expressed as

$$K = \frac{\left[M_x O_y\right]}{\left[M\right]^x \left[O_2\right]^{y/2}}$$

The standard free energy change ΔG^0 can be computed from the following relation,

$$\Delta G^0 = -RT \ln K_p = -RT \ln \frac{1}{p_{O2}}$$

Where R is the universal gas constant, T is the absolute temperature and K_P the equilibrium constant of the reaction. Thermodynamically, the reaction is governed by the standard free energy change ΔG^0 which must be negative for spontaneous reaction to take place. In order to control the oxidation reaction the temperature and the partial pressure of O_2 have to be controlled.

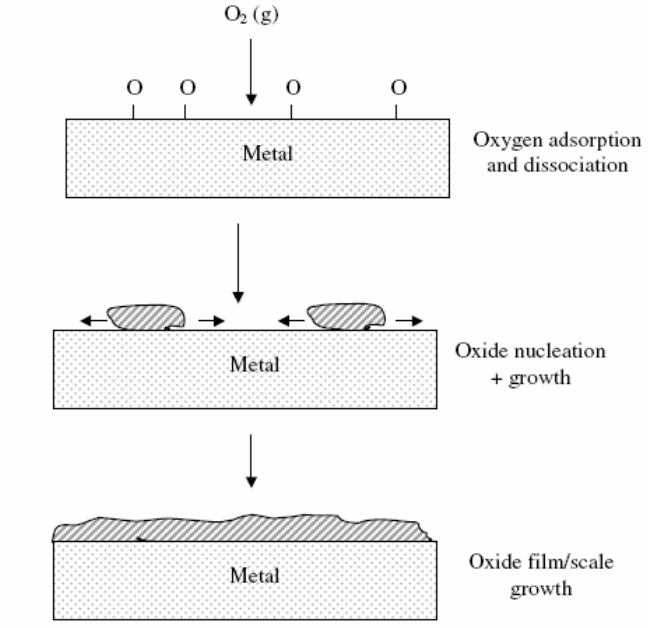

Figure 13. The formation of the oxide film at the surface of metals (Addepalli *et al*., 2000)

Moreover if we refer to the definition of the standard free energy of formation,

$$\Delta G_f^0 = \Delta H_f^0 - T\Delta S_f^0$$

where ΔG_f^0 is the standard enthalpy of oxide formation and ΔS_f^0 the standard entropy. At a temperature above the melting point of the metal, the free energy change ΔG_f^0 increases since the reaction in a liquid state involve a higher entropy change.

This set of experiments showed that metal foam can be formed and stabilized thanks to the oxidation of the bubble surface since the foaming did not form with argon only. Thus, the oxide layer forming at the gas/bismuth alloy interface around the bubbles plays a significant role in stabilizing the foam. This can be attributed to different phenomena

- Oxidation decreases the surface tension and thus stabilizes the bubbles.
- some oxide particles are formed and stabilize the bubbles as observed with other types of particles (Kaptay, 2003).
- an oxide layer is formed on the bubble surface and acts like a shell. The oxide film formed on the inner surface apparently help to stabilize the cells against coarsening and coalesce (Gergeley *et al*., 2003).

The last phenomenon is the most probable. Indeed, when the oxygen was directly injected in the metal, the foam was stabilized. However, when the oxygen was delivered on the top of the melt, a crust formed. If some argon was injected in the liquid metal a pocket of gas formed underneath this crust because the bubbles injected coalesced rapidly since the necessary oxide layer was not formed. Therefore, the oxygen has to be injected directly inside the liquid metal. If this injection is combined

with the oxide crust formation on the top, the bubbles injected and stabilized by the oxide shell, rise to the surface by buoyancy and accumulate under the crust. This corroborates results reported by Babcsan *et al*.(2003). The authors showed in comparing the foam elaborated by air, oxygen and nitrogen injection in aluminum alloys that the oxide layer prevented the coalescence and helped stabilize the bubbles.

Effect of the Melt Temperature

For Alloy 1, the different experiments were carried out in the liquid state (100-150ºC). In this state, the foaming occurred with hot gas injection. However, the foam obtained was very brittle and essentially composed of ceramic due to the high temperature of the gas promoting oxidation. Therefore, in the liquid state a high degree of oxidation is needed to obtain stable foam, so that an oxide solid shell is formed around the bubbles.

In contrast, foaming did not occur with Alloy 3 in the liquid state at high temperature. Instead, a black powder was quickly formed and released. However, foaming occurred when the alloy was in the semi-solid region at temperatures under 150ºC accompanied by a mechanical stirring, and injection of cold air. Then, increase in viscosity associated with the oxidation of the cells walls promoted foam stabilization.

Effect of the Gas Temperature

As previously explained, the process of oxidation is thermally activated. Thus, the temperature of the gas at the gas/melt interface is essential. But the effect of the temperature depends also on the alloy composition. Some alloying elements are oxidized more easily than others. For Alloy 1, in the liquid state, we observed a different behavior between injecting hot or cold air. When the gas was cold, a few bubbles formed but were not stable because the oxidation layer around the bubbles was probably not sufficient to prevent the coalescence. This explains why a pocket of gas was formed underneath the oxidized top layer (Fig. 12). When we injected a mixture of argon/air at 100ºC, metal oxidation was more significant and solid foam essentially composed of ceramic was formed. This foam was very brittle because it was mainly composed of ceramic. Therefore temperature of the gas must be carefully controlled to oxidize sufficiently but not excessively to stabilize the bubbles and form strong foam structure.

Moreover, the gas mixture does not need to be heated when injected in alloy in the semi-solid state. Heating the gas mixture prior to injection makes the oxide layer thicker and the foam more stable. As a result, if the oxide layer formed around the bubble is stronger, the coalescence of the bubbles should be inhibited and we can expect smaller cells in the solid foam.

Effect of the Alloy Composition

Alloys 1 and 3 are both composed of bismuth, lead, and tin in similar amounts. These alloys differ in the fourth major element which is cadmium for Alloy 1 and antimony for Alloy 3. Let us consider the standard electrochemical potential of the different metals. In general, the metal plays the role of anode in the oxydo-reduction reaction

$$M \rightarrow M^{n+} + n\, e^{-}$$

The electrochemical potential is measured in solution with respect to the standard hydrogen electrode. The potential represents the affinity of the metallic element for oxygen. In other words, the higher the potential the easier the metal will be oxidized. Table 5 summarizes the standard potential of the elements present in the alloys used in the present study. It indicates that in Alloy 1, the Cadmium will react first to form the cadmium oxide CdO. The electrochemical potential of tin is

slightly larger than that of lead and tin should react first in Alloy 3. Note that the tin can form stannic oxide, SnO_2, or stannous oxide SnO. Table 5 clearly established that the two alloys behave differently and Alloy 1 will oxidize more easily than Alloy 3 thanks to the presence of cadmium which has a stronger affinity for oxygen than antimony. In addition, some complex oxides can form. Experimentally, foam was produced from Alloy 1 in liquid state. This was not possible with Alloy 3 because oxide powder was quickly formed. The foam formed with Alloy 1 was composed in major part with ceramic since it was very brittle. To explain the experimental evidences, the difference in operating temperatures used (120ºC for Alloy 1 and 230ºC for Alloy 3) must be considered. The larger temperature for Alloy 3 can explain the rapid formation of oxide powder. It would be interesting to analyze the surface of the cell in XPS or Auger spectroscopy in order to determine the composition and the thickness of the oxide layer stabilizing the foam. However, this falls beyond the scope of this study.

Moreover, one must also consider the permeability of this oxide layer to oxygen. Indeed the oxide layers act like a protection for the metal. The thickness of this oxide layer and the oxidation kinetic depend on the diffusion properties of oxygen through the oxide layer. In the case of aluminum, the oxide layer formed is relatively thin, in the gas injection method the thickness of the oxide layer is about 10 and 60 nm (Babcsan *et al*., 2003). The oxide layer of aluminum has a low permeability to oxygen that is why aluminum is resistant to corrosion. So the thickness of the oxide layer formed with aluminum might not be sufficient to stabilize the foam by this process. However, Babcsan *et al*. (2003) experimentally showed that the oxygen plays an evident role in the aluminum foam stabilization but did not provide any physical explanation. He noted a 30 nm thick oxide layer allowed preventing the cell walls rupture. Babscan *et al*.(2004), added that the oxide layer thickness depend on the time. That is why, it would be interesting in the development of this process to study the effect of the stirring and gas injection time. One can add that the oxidation of aluminum is generally increased by alloying elements such as sodium, lithium, calcium and magnesium (Bergsmark *et al*., 1989).

Table 5. Electrochemical metals standard potentials.

Metal	Potential, Volts	Metal	Potential, Volts
Potassium	2.92	Tin	0.136
Sodium	2.71	Lead	0.122
Calcium	2.2	Hydrogen	0
Magnesium	1.87	Antimony	-0.19
Aluminum	1.3	Arsenic	-0.32
Manganese	1.07	Bismuth	-0.33
Zinc	0.758	Copper	-0.345
Chromium	0.6	Mercury	-0.799
Iron	0.441	Silver	-0.8
Cadmium	0.398	Platinum	-0.863
Nickel	0.22	Gold	-1.1
Cobalt	0.29		

Powder Formation

When a significant amount of oxygen is entrapped due to stirring in air, the thin barrier separating the bubbles undergoes significant surface oxidation. When the struts between the bubbles becomes too weak to withstand the liquid metal surface tension forces and break as illustrated in Fig. 14(a) (Riviello *et al*., 1994). We effectively observed this phenomenon with Alloy 1 after more than 6 minutes of stirring at 7000 rpm. The foam obtained was black and very brittle. Figure 14(b) shows the evolution of the foam cells with the increasing oxidation. The morphology of the foam changed as time passes due to oxidation. As a result, the foam becomes more brittle and more and more black. One can see the morphology changes of the edges. On the second picture the edges started to break and one the third picture, a part of the edges are gone.

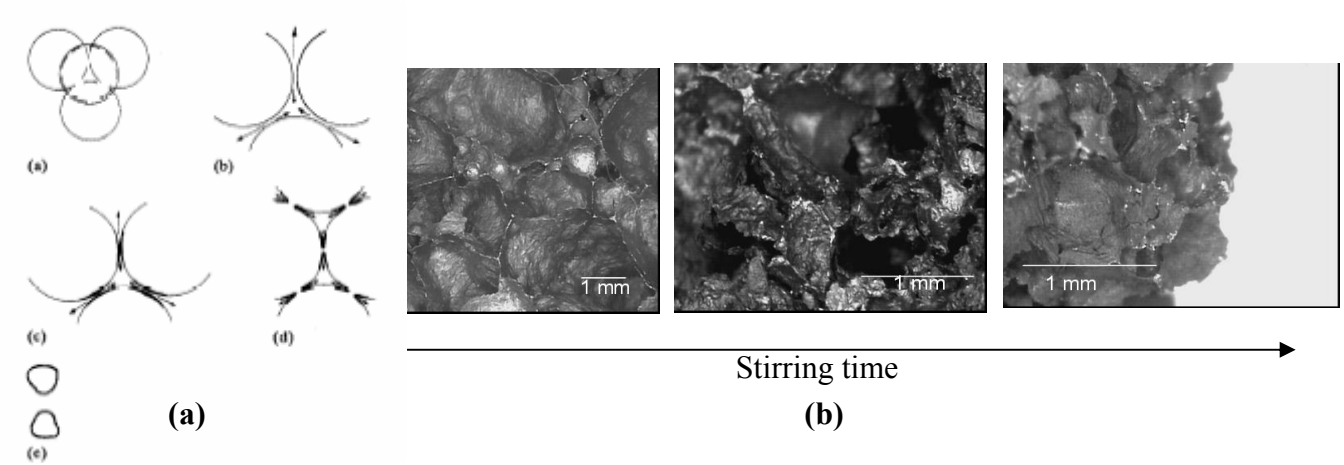

Figure 14. **(a)** powdering mechanism (Riviello *et al*., 1994) and **(b)** evolution of the foam cells with time.

Figure 15 shows the SEM micrograph of one edge of the most oxidized sample covered with 500 nm particles. This foam crumbled by routine handing.

Moreover, the formation of powder increased with the temperatures of both the metal and the injected gas. As a result, we did not observe any powder when we injected cold gas in Alloy 1. For Alloy 3, the powder was formed immediately after stirring and the more we stirred the more the powder was released from the liquid metal without air injection. However, at 150ºC (in the semi-solid state), powder formation was not observed. Therefore, powder formation is a thermally activated and depends on the nature of the oxide formed.

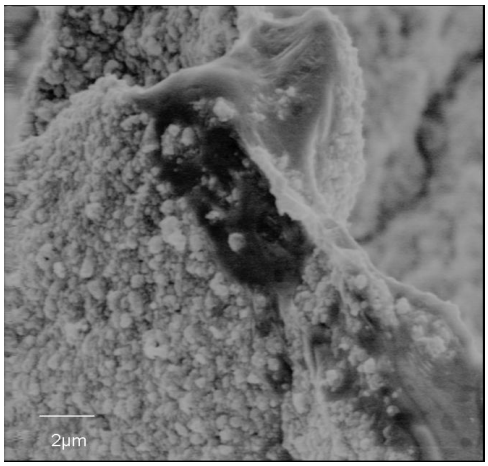

Figure 15. SEM micrograph of the most oxidized sample.

Effect of the Baffles

The role of the baffles is to break the bubbles injected and those formed by breaking waves generated during stirring. The bubbles are in the order of 1 to 5 mm in diameter, with some bigger bubbles of 10 to 15 mm due to the coalescence. However we can observe some very small bubbles with a size less than 1mm around some big bubbles. Therefore, we can assume that the baffles play effectively a major role in breaking the bubbles. Moreover we realized the effect of the baffles when we stirred the molten metal contained in Pyrex vessel in argon atmosphere. We were able to see the small gas bubbles compressed between the baffles and the Pyrex vessel rising up at the surface and burst. Moreover, the way air is injected (200 cc/min through a 55 mm diameter pipe) can partially explain the presence of large bubbles and needs to be optimize. The system could be improved in using a vibrating nozzle which could inject separate bubbles with a controlled size.

To better appreciate the effect of the baffles, an experiment should be performed without the baffles stirring Alloy 3 at 6000 rpm at temperature 145°C in ambient atmosphere with argon/air mixture injection at 200 cc/min of air. From our previous arguments about the role of oxidation and the semi-solid state of the alloy in the foam stabilization, foam should be formed and if the baffles play the role we think, the bubble size should be bigger.

Effect of Cooling Procedure

To examine the effect of the cooling rate, we cooled the foam by two different ways: (i) by air, (ii) by quenching with liquid nitrogen. Then we compared the solid foams obtained by the two methods. We expected to see smaller bubbles because of the coalescence which can occur during a long solidification process (Yang and Nakae, 2003). But we did not observe a significant difference between the two samples expect a smaller bubbles number. But it is not significant enough to draw some conclusions. The coalescence probably occurred in major part during the stirring when the bubbles rose up at the surface.

Figure 16. Foam made of Cerromatrix^{TM} alloy.

Evaluation of the Foam Density and Porosity

Figure 16 shows the photograph of a typical example of metal foam synthesized during this project. Two measurements of densities were made:

1) A cube of metal foam was cut. The volume was estimated from the dimensions and the mass measured with an accurate balance. The density was found to be 1.7 g/cm^3 corresponding to a porosity of 81%.
2) The foam sample was covered with adhesive tape and placed in a graduate beaker filled of water. The foam volume is equal to the volume of water displaced. The density was measured as 1.9 g/cm^3 corresponding to a porosity of 80%.

Both methods gave similar value of density and porosity equal to 1.8 g/cm^3 and 80%, respectively.

4.3 Comparison with Existing Gas Injection Processes

Experimental data and conclusions about the effect of the different parameters for metal foaming by direct gas injection process were difficult to find in the literature. To the best of our knowledge, discussion of the effects of important parameters such as the gas flow rate, the stirring rate, and ways of introducing the particles have not been reported. The Cymat and Hydro process consist in injecting gas (nitrogen, air, argon) in an aluminum melt with a uniform distribution of ceramic particles. Gas is added under the surface of the melt using a rotating impeller designed to produce small bubbles as illustrated in Figure 17 (Curran, 2001). According to Banhart (2001), the concentration of the particles ranges from 5 to 20% and their size from 5 to 20 μm. The foam thickness obtained is about 10 cm thick, the porosity varies from 80 to 98%, the cell size from 25 to 3 mm and the wall thickness from 50 to 85 μm. Unfortunately, the author did not discuss the stirring rate and the gas flow rate. According to Deqing and Ziyuan (2003), the stirring rate might be in order of 1,000 rpm and the gas flow from 0.5 to 1 L /min for an unspecified melt size.

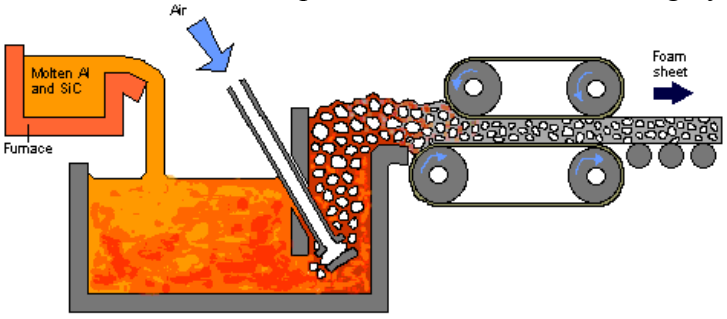

Figure 17. Cymat and Hydro process (Curran, 2001).

Our process differs from the direct gas injection process as follows:

1) The foam is formed and stabilized without adding particles. This offers a practical and financial advantage.
2) We use baffles to break the bubbles in order to break the bubbles and reduce their size.
3) We formed the foam at 150ºC with an alloy presenting a semi-solid interval from 102 to 226 ºC.
4) The foam is stabilized by oxidation of the melt. This might also be the case for the Cymat process.
5) We stirred the metal at high velocity which can promote a favorable globular microstructure in the semi-solid sate.

The foam produced in the present study was 6 cm thick, the porosity was about 80%, and the cell diameter varied from less than 1 mm to 15 mm. The cell diameter can be decreased by optimizing the gas injection system through the use: i) smaller gas injection pipe, and ii) a vibrating system which would allow injecting separate bubbles.

According to Curran (2001), attempts have been made to use alloys which do not require the addition of solid particles. In one case, a 91% Mg-9% Al alloy was stirred rapidly at a temperature between the solidus and liquidus temperatures, producing a viscous dendritic melt, to which argon gas was added. In general, such attempts have been unsuccessful, only producing metals with up to 20% porosity. The main difficulty lies in maintaining a uniform temperature within a very narrow range. If the temperature is too low the melt is too viscous to be processed, and if the temperature is too high the dendrites in the melt do not grow sufficiently quickly, and the melt is not sufficiently viscous to trap the gas. It can also be difficult to produce dendrites which are sufficiently fine to generate slurry on the scale of the cell wall thickness.

In the present study, we managed to synthesize foam with 80% porosity from an alloy commercially available under the name Cerromatrix™ (48% Bi, 28.5% Pb, 14.5% Sn, and 9% Sb) in the semi solid state and by injecting air. The Cerromatrix™ alloy used to develop this process had poor mechanical properties and a low melting temperature. However, it enabled process development and the definition of key process parameters while working at low temperature. In order to expand this process to aluminum foam it would be interesting to compare the surface tension and the viscosity properties in the semi-solid state of the aluminum alloy with these of the bismuth alloy considered. We should also compare the thickness of the oxide layer formed.

5. CONCLUSION AND RECOMMENDATIONS

5.1 Conclusion

The following conclusions can be drawn from our study:

1) The oxide layer formed at the interface Gas/Bismuth alloy around the bubbles plays an evident role in the foam stabilization. This oxide layer acts like a shell around the bubble and prevents bubble coalescence. In addition, the oxide crust formed on the melt free surface prevents the bubbles from bursting.
2) The foaming of the cerromatrix alloy occurred at 150ºC. At this temperature the alloy was in semi-solid state resulting in a higher melt viscosity. This increase in viscosity associated with the oxidation of the cells walls promoted the foam stabilization.
3) Oxide powder is released from the liquid metal by breaking the lamellae oxidized by the entrapped air. This phenomenon depends on (i) the alloy composition, (ii) the alloy temperature, (iii) the gas temperature, (iiii) the stirring rate, and (iiii) the stirring time.
4) Melt oxidation increases with the gas temperature as it is a thermally activated process. As a result foam could be obtained with Alloy 1 in liquid state with hot gas injection. However, this foam was very brittle because of large oxidation state.

5) The alloy composition plays a role by the difference in the oxide layer formed. The larger the electrochemical potential of the metallic constituents the more likely the alloys will foam.
6) The porosity of the foam elaborated is about 80%, the cell diameter from less than 1mm to 15 mm.

Finally, the objective of producing microfoam has not been reached. However, a new process has been developed to elaborate metal foam from Cerromatrix™ alloy (48% Bi, 28.5% Pb, 14.5% Sn, 9% Sb) and cerrosafe™ alloy (48% Bi, 28.5% Pb, 14.5% Sn, 9% Sb). The process consists of injecting a controlled amount of air in molten metal contained in a baffled beaker while stirring at high speed (> 5,000rpm). The process presents the following advantages: (i) foam is stabilized without addition of oxide or carbide particles, (ii) large blocks of raw materials can be used as opposed to fine powder. This results in practical and financial benefits as particles may be costly and difficult to incorporate in the metallic matrix. However, the project was not successful at producing microfoams as observed with aqueous solutions. The possibility of producing metallic microfoams but optimization and improvement of the process is required.

5.2 Recommendations

The process developed in this study can be improved by following some recommendations derived from our experience.
1. In order to improve and better understand the foaming process the following experiments should be performed:

- Run an experiment without baffles to understand their effect.
- Analyze the composition and thickness of the oxide layer formed at the bubble surface by XPS or Auger spectroscopy.
- Improve the air injector by reducing the pipe diameter and injecting separate bubbles possibly thanks to a vibrating system as performed in the Cymat process.

2. In order to extend this process to aluminum alloys, the following properties should be compared:

- Rheological properties in the semi-solid state
- Surface tension of the metal in air in liquid and semi-solid states
- The thickness and microstructure of the oxide layer formed in contact with air
- The microstructure dendrite/globular.

3. Extension of the developed process to larger scales will face some challenges. Indeed, scale up will be limited by the size of the mixer and its power consumption which could affect process cost and reliability. To overcome these challenges a continuous process could be developed by feeding the container from the bottom and extracting the foam at the top.

6. REFFERENCES

Addepalli, S., 2000. *High-Temperature corrosion of Aluminum Alloys*: *Oxide alloy interactions and sulfure interface Chemistry*. PhD Thesis, University of North Texas, Denton, TX.

Asthana, R., 1993. *Stability of heterogeneous particles at fluid interfaces in composite slurries*. Scripta Metallurgica et Materialia, Vol. 29, No10, pp. 1261-1266.

Babscan, N., Letimeier, D., and. Degischer, H.P., 2003. *Foamability of particle reinforced Aluminum Melt.* Ma.-wiss. U.werstoffech. Vol. 4, pp. 22-29.

Babscan, N., Leitmeier, D., Degischer, H.P., and Banhart, J., 2004. *The role of oxidation in blowing particle-stabilised Aluminum foams*. Advanced Engineering Materials, Vol. 6, pp. 421-428.

Banhart, J., 2001. *Manufacture, characterization, and application of cellular metals and metal foams*. Progress in Materials Science, Vol.46, pp. 559-632.

Bergsmark, E., Simensen, C.J., and Kofstad, P., 1989. *The Oxidation of Molten Aluminum. Material science and Engineering* A, Vol. 120-121, No 1, pp. 91-95.

Bhakta, A. Ruckenstein, E., 1997. *Decay of standing foams: drainage, coalescence and collapse*. Advances in Colloid and Interface Science, Vol. 70, pp. 1-124.

Boris, Y. A., 1997. *Power Actuation System of Minimal Energy Consumption for Aircraft*. International Science and Technology Center. Promising Research Abstract PRA-3113.

Braccini, M., Martin, C.L, Tourabi, A., Brechet , Y., and Suery, M., 2002. *Low shear rate behavior at high solid fractions on partially solidified Al-8wt.% Cu alloys*. Materials Science and Engineering, Vol. 337, No 1-2, pp.1-11.

Binks, B.P., 2002. *Particles as surfactants—similarities and differences*, Current Opinion in Colloid & Interface Science, Vol. 7, No 1-2, pp. 21-41.

Curran, D.,2001. *Metal foam*. http://www.msm.cam.ac.uk/mmc/people/dave/dave.html

Deqing, W. and Ziyuan, S., 2003. *Effect of ceramic particles on cell size and wall thickness of aluminum foam*, Materials Science and Engineering A, Vol. 361, No1-2, pp. 45-49.

Eustathopoulos, N., Drevet B. and Muolo M. L, 2001. *The oxygen-wetting transition in metal/oxide systems***.** Materials Science and Engineering A, Vol. 300, No 1-2, pp. 34-40.

Eustathopoulos, N. and Dervert, B., 1994. *Interfacial bondings, wettability and reactivity in metal/oxide system*. Journal of Physics Vol. 3, France No4, pp. 1865 -1881.

Gergeley, V., Curran, D.C and Clyne, T.W. 2003. *The FOAMCARP process: foaming of Aluminum MMCs by the chalk- Aluminum reaction in precursors*. Composite Science and Technology, Vol. 63, No 16, pp. 2301-2310.

Giuranno, D., Gnecco, F., Ricci, E.and Novakovic, R. 2003. *Surface tension and wetting behavior of molten Bi-Pb alloys*. Intermetallics Vol. 11, No 11-12, pp.1313-1317.

Hur, B-Y., Park, S.-H., and Hiroshi, A. 2003. *Viscosity and surface tension of Al and effects of additional element*, Materials Science Forum, ISEPD - International symposium on Eco-Materials Processing & Design N°4, Gyungpodae, Korea, April 02, 2003, vol. 439, pp. 51-56.

Hashim, J.,.Looney,L. and. Hashmi, M.S.J., 2002. *Particle distribution in cast metal matrix composites Part 1 and 2*, Journal of materials Processing Technology, Vol. 1239, No 2, pp. 251-257.

Ip, S.W., Wang, Y., and Toguri, J.M., 1999. *Aluminum foam stabilization by solid particles*. Canadian Metallurgical Quarterly, Vol. 38, No1, pp. 81-92.

Johansson, G. and Pugh, R.J., 1992. *The influence of particle size and hydrophobicity on the stability of mineralized froths*, International Journal of Mineral Processing, Vol. 34, pp. 1–21.

Kaptay, G., 2003. *Interfacial criteria for stabilization of liquid foams by solid particles.* Colloids and Surfaces A: Physicochemical and Engineering Aspects, Vol. 230, No1-3, pp. 67-80.

Koke, J., Modigell, M., 2003. *Flow behaviour of semi-solid metal alloys*. Journal of Non-Newtonian fluid Mechanics, Vol. 112., No 2-3, pp. 141-160

Kumagai, H., Torikata, Y., Yoshimura, H., Kato, M., and Yano, T., 1991. *Estimation of the Stability of Foam Containing Hydrophobic Particles by Parameters in the Capillary Model(Food & Nutrition)*, Agricultural Biological Chemistry, Vol. 55, No7, pp. 1823–1829.

Kurian, L. and Sasikumar, R., 1992. *Redistribution of second phase particles in solidifying alloy melts—entrapment and microsegregation within dendritic networks*. Acta Metallurgica et Materialia, Vol. 40, No 9, pp2375-2379.

Naidich J. V.: 1981. in *Progress in Surface and Membrane Science*, D.A. Cadenhead and J.F. Danielli, eds., Academic Press, New York, NY, pp. 353–484.

Paquot, M., 2004. *Approche pluridisciplinaire des tensioactifs et de leurs propriétés*. Université de Genoux (Belgique), unité de chimie biologique industrielle.

Prasad, L. C. and Mikula, A., 1999. Role *of surface properties on the wettability of Sn–Pb–Bi solder alloys*, Journal of Alloys and Compounds, Vol. 282, No 1-2, pp. 279-285

Riviello, A.E., Young, D. and Sebba, F., 1994. *A novel method of finely divided tin metal powders.* Powder technology, Vol. 78, pp19-24.

Sebba, F., 1987. *Foams and Biliquid Foams – Aphrons*. John Wiley & Sons, New York, NY.

Sosnick B., 1948. *Process for making foam like mass*, US Patent 2,434,775, Jan. 20 1948.

Suery, M. 1996. *Mise en forme à l'etat semi-solide: rhéoformage and tixoformage*, Techniques de l'ingénieur, Report no. M612. http://www.techniques-ingenieur.fr

Sukumaran, K., Pai, B.C, Chakraborty, M., 2004. *The effect of isothermal mechanical stirring on Al-Si alloy in the semisolid state condition*. Material Science and Engineering, A, Vol. 369, No1-2, pp- 275-283.

Taylor, J.W. ,1956. *The surface tension of liquid metal*, Acta Metallurgica, Vol. 4, No5, pp. 460-468

Tham, LM., Gupta, M., and Cheng, L., 1999. *Influence of processing parameters on the near-net shape synthesis of aluminum-based metal matrix composite*, Journal of Materials Processing Technology, Vol. 89-90, pp. 128-134

Wilde, G. and Perepezko, J. H., 2000. *Experimental study of particle incorporation during dendritic solidification*. Materials Science and Engineering A, Vol. 283, No 1-2, pp. 25-37.

Wu, S., Wu, X., Xiao, Z., 2004. *A model of growth morphology for semi-solid metal*s. Acta Materialia, Vol. 52, No12, pp. 3519-3524.

Wübben, Th., Stanzick, H., Banhart, J., and Odenbach, S., 2003. *Stability of metallic foams studied under microgravity*, Journal of Physics: Condensed Matter, Vol.15, pp. 427-433.

Yang, C.C and Nakae, H., 2003. *The effects of viscosity and cooling conditions on the foamability of Aluminum alloy*. Journal of Material Processing Technology, Vol. 141, pp. 202-206.